ACS OMEGA

Article

Cite This: ACS Omega 2018, 3, 12722−12729

http://pubs.acs.org/journal/acsodf

Bioinspired Environmentally Friendly Amorphous $CaCO_3$-Based Transparent Composites Comprising Cellulose Nanofibers

David Kuo, Tatsuya Nishimura,† Satoshi Kajiyama, and Takashi Kato*

Department of Chemistry and Biotechnology, School of Engineering, The University of Tokyo, 7-3-1 Hongo, Bunkyo-ku, Tokyo 113-8656, Japan

Supporting Information

ABSTRACT: Amorphous calcium carbonate (ACC) stabilized by acidic macromolecules is a useful material for the development of environmentally friendly composites. In this study, we synthesized transparent and mechanically tough ACC-based composite materials by the incorporation of water-dispersible cellulose derivatives, namely, carboxymethyl cellulose (CMC) and surface-modified crystalline cellulose nanofibers (CNFs). A solution mixing method used in the present work proved to be a powerful and efficient method for the production of mechanically tough and environmentally friendly materials. Molecular-scale interactions between carboxyl groups and Ca^{2+} ions induce homogeneous dispersion of CNFs in the composites, and this gives composite films with high transparency and high mechanical properties. The composite films of CMC, CNFs, and ACC at the mixture ratios of 40, 40, and 20 wt %, showed high mechanical properties of 15.8 ± 0.93 GPa for the Young's modulus and 268 ± 20 MPa for the tensile strength. These designed materials that are based on ACC may open up new opportunities in many fields in applications that require the use of environmentally friendly, biodegradable, mechanically tough, and transparent composite materials.

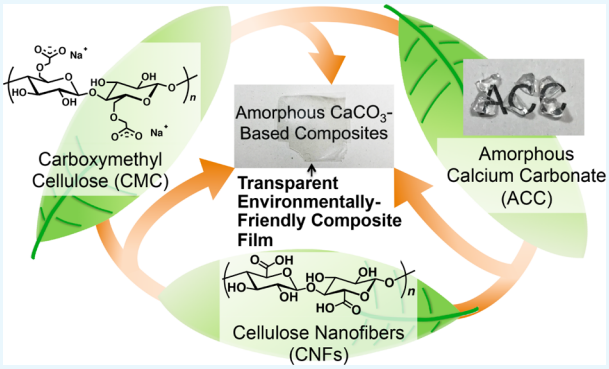

INTRODUCTION

Material manufacturing with environmentally friendly resources is important because of the rising demands for sustainability.[1−9] Material scientists can be inspired by nature in the design of new environmentally friendly materials.[10−16] In particular, biomineralization-inspired materials have attracted much attention because of the formation of nano- to centimeter-scale controlled hierarchical hybrid structures under mild conditions. Such biomineralization-inspired materials play important roles and bring a new concept into the fields of material syntheses.[17−32] Various approaches to mimicking such layered composite structures have been reported.[11,12,30−32] Biominerals consist of organic matrices, for example, polysaccharides such as chitin and cellulose, and inorganic components such as $CaCO_3$, calcium phosphate, hydroxyapatite, and silicate.[1,2] These components are all considered to be environmentally friendly in terms of materials science and technology. For $CaCO_3$-based materials, the nacre of shells is a representative composite. It forms mechanically tough organic/inorganic layered structures under ambient conditions. This structure is based on the aragonite phase. These materials are hard and nontransparent composites because the ratio of organic to inorganic matter is 5 to 95 wt %. In contrast, the exoskeletons of crustaceans are more flexible and more transparent because of the higher contents of organic substances. They consist of hydrated amorphous calcium carbonate (ACC), proteins, and chitin fibers. Our intention here is to develop flexible, tough, and transparent composites by mimicking the exoskeletons of crustaceans.

In nature, ACC is a useful transient state of crystalline phases such as calcite and aragonite.[33−37] In the preparation of synthetic $CaCO_3$-based materials, ACC has been used to control the morphologies of the resultant crystalline phases.[38,39] Recently, we also used colloidal ACC for the preparation of liquid crystal nanorods.[40] Composites based on stable ACC are expected to be transparent and mechanically tough in all directions.[14,41] We found that an acidic polymer, poly(acrylic acid) (PAA), acts as a stabilizer for ACC, providing ACC-based composites that have significant stability for years under ambient conditions.[14,41] We developed stable ACC-based transparent composites in a previous study.[41] These composites were brittle in the bulk state, but stable thin-film coatings were achieved.[41] In our previous paper,[14] we described that we introduced cellulose nanofibers (CNFs) with acidic groups into these materials, which enabled the preparation of mechanically stable thin-film materials.[14] These materials were prepared by immersion of bacterial cellulose into an ACC colloidal solution.[14] The preparation of

Received: August 13, 2018
Accepted: September 13, 2018
Published: October 5, 2018

DOI: 10.1021/acsomega.8b02014
ACS Omega 2018, 3, 12722−12729

transparent films by using biobased materials such as CNFs and chitin has attracted attention.[42−46] However, only a few studies of the introduction of ACC into these CNF-based materials have been reported.[14,29] Transparent, mechanically tough, and environmentally friendly composite materials are expected to contribute significantly to the sustainable development of composites in the field of material engineering.

Here, we describe a new approach to the development of mechanically tough and transparent ACC-based composite materials containing cellulose derivatives. The method involves tuning the compatibilities among four components, namely, carboxymethyl cellulose (CMC), which interacts with calcium ions, CNFs, and ACC/PAA at the molecular- and nanoscale-levels (Figure 1). We also discuss the effects of the amount of ACC incorporated into the cellulose matrices on the transparency and mechanical properties.

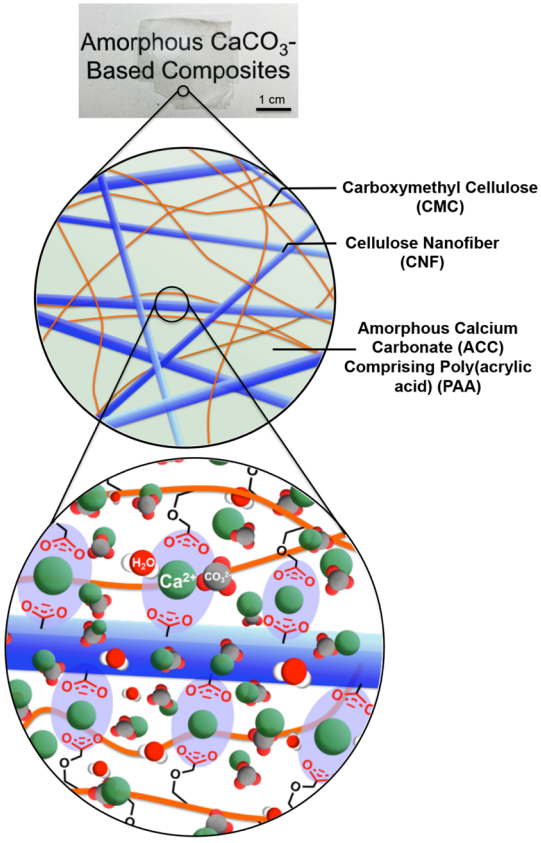

Figure 1. Schematic diagram of the development of transparent films with biomimetic structures.

RESULTS AND DISCUSSION

Mechanically Tough and Transparent Composite Films of CMC, CNF, and ACC. Transparent cellulose-based ACC composite materials were obtained using CMC as an organic matrix. CMC was expected to provide fundamental physical properties to the composites. Surface-carboxylated CNFs with 2,2,6,6-(tetramethylpiperidin-1-yl)oxyl (TEMPO) were introduced into the composites to enhance the mechanical properties of the transparent films.

CMC, CNFs, and ACC stabilized by PAA were homogeneously dispersed in aqueous solution. The dimension of the TEMPO-oxidized CNFs was estimated to be ca. 20 nm in diameter and micrometer-scaled length with transmission electron microscopy (TEM) (Figure S1). The homogeneous dispersion of CNFs with negative surface charges is crucial in the formation of homogeneous structures comprising four components, that is, CMC, CNFs, and ACC including PAA. Transparent thin films were obtained by drying a mixed solution of the four components in an acrylonitrile butadiene styrene (ABS) case. The composition of the prepared CMC/CNF/ACC composite films is shown in Table 1.

Table 1. Component Ratios of the Prepared Samples

samples	CMC (wt %)	CNF (wt %)	ACC (wt %)
50/50/0 (CMC/CNF/ACC)	50	50	0
45/45/10 (CMC/CNF/ACC)	45	45	10
40/40/20 (CMC/CNF/ACC)	40	40	20
35/35/30 (CMC/CNF/ACC)	35	35	30
100/0/0 (CMC/CNF/ACC)	100	0	0
87/0/13 (CMC/CNF/ACC)	87	0	13
80/0/20 (CMC/CNF/ACC)	80	0	20
71/0/29 (CMC/CNF/ACC)	71	0	29

The X-ray diffraction (XRD) patterns of the CMC/CNF/ACC composite films show no peaks attributable to $CaCO_3$ crystalline phases (Figure 2), indicating high stability of ACC

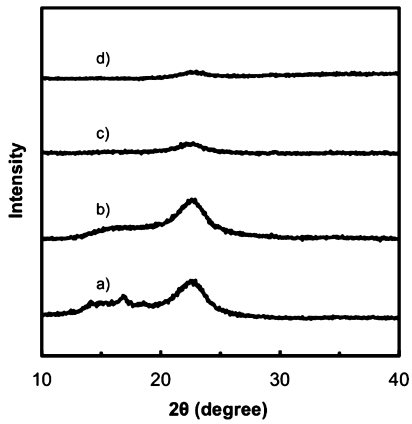

Figure 2. XRD patterns of composites with CMC/CNF/ACC ratios: (a) 50/50/0 wt %, (b) 45/45/10 wt %, (c) 40/40/20 wt %, and (d) 35/35/30 wt %.

under ambient conditions. A peak from the ACC phase appears in the IR spectra of the CMC/CNF/ACC composite films (Figure 3). The Fourier-transform infrared (FT-IR) absorption peak at 866 cm^{-1}, which is attributed to the ν_2 out-of-plane bending of CO_3^{2-}, confirms the presence of ACC in the hybrid.[40] These results suggest that CNF incorporation into the composites by the solution mixing method does not disturb the homogeneous structures of the cellulose derivatives and ACC. It should be noted that the four components of the CMC/CNF/ACC composite films have high transparencies (Figure 4). CNF incorporation does not significantly reduce the transparency of the composite thin films in the visible-light region. Homogeneous composite films of cellulose derivatives and ACC were expected to have high transparency because the refractive indices $\tilde{n}$ of $CaCO_3$ and cellulose are similar ($CaCO_3$ $\tilde{n} \approx 1.58$, cellulose $\tilde{n} \approx 1.56-1.60$).[47−49] The transparency remains high at above 80% transmittance even with the

DOI: 10.1021/acsomega.8b02014
ACS Omega 2018, 3, 12722−12729

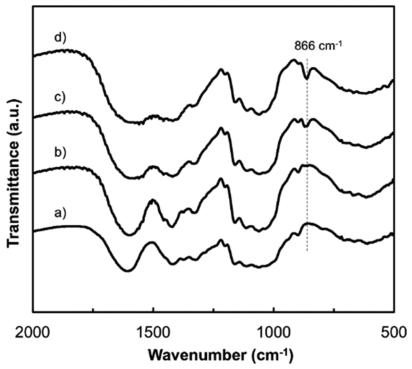

Figure 3. IR spectra of CMC/CNF and the CMC/CNF composite with ACC: (a) CMC/CNF/ACC = 50/50/0 wt %, (b) 45/45/10 wt %, (c) 40/40/20 wt %, and (d) 35/35/30 wt %.

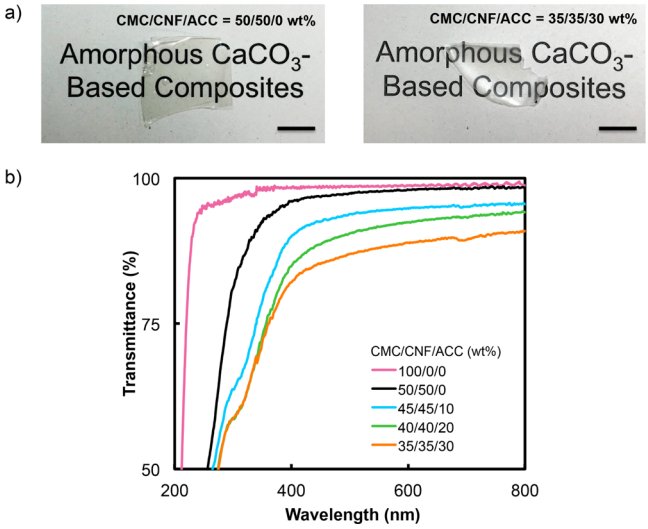

Figure 4. (a) Photographs of CMC/CNF composites containing 0 and 30 wt % ACC, scale bar = 1 cm and (b) UV−vis spectra of CMC/CNF and CMC/CNF/ACC composite materials.

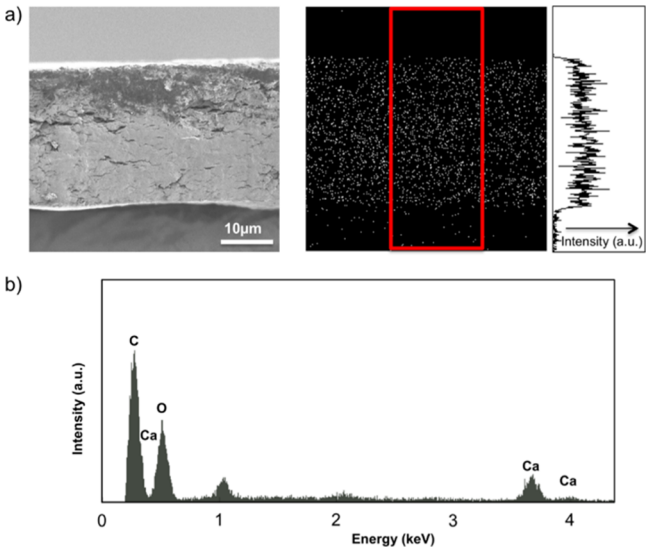

Figure 5. EDX results for CMC/CNF/ACC at ACC = 30 wt %: (a) SEM image of the cross section (left) and Ca^{2+} Kα X-ray elemental mapping of the material (right) and (b) EDX spectrum corresponding to the cross section of the CMC/CNF/ACC material shown in (a).

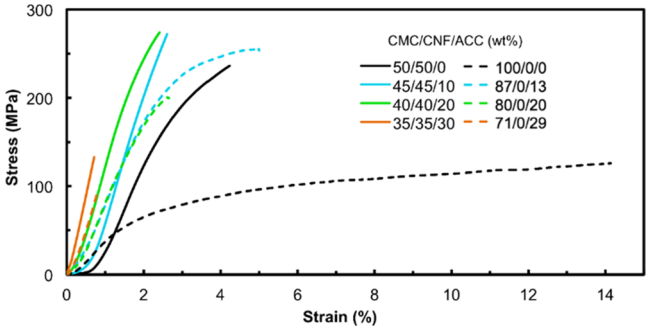

Figure 6. Mechanical properties of CMC/CNF/ACC and CMC/ACC composite materials at different ACC content ratios.

introduction of 30 wt % ACC into the polymer. Highly transparent composite materials were obtained because the refractive indices of cellulose and ACC are similar.

The composite structures of the CMC/CNF/ACC films were examined by scanning electron microscopy (SEM) observation of the fracture surface of the CMC/CNF/ACC composites containing 30 wt % ACC (Figure 5a, left). Elemental analyses with energy-dispersive X-ray spectroscopy (EDX) were also conducted (Figure 5a, right). The SEM image shows homogeneous structures without aggregation of any of the components (Figure 5a, left). EDX mapping of the composites shows homogeneous distribution of Ca atoms in the composite film (Figure 5a, right). These results suggest that no domain boundaries are formed at macroscale in the composite films. Because of this homogeneous structure, the composite films exhibit no light scattering and high transparency. The similarity between the refractive indices of ACC and cellulose derivatives contributes to the suppression of light scattering.

The transparent CMC/CNF/ACC composites prepared by a solution mixing method in this study gave high mechanical performances. The mechanical properties of the four-component films were enhanced by ACC incorporation. Figure 6 presents the stress−strain curves for the composite films containing various amounts of ACC. A summary of mechanical properties is given in Table 2. The CMC/CNF composite films had a Young's modulus and tensile strength of 10.7 ± 1.2 GPa and 240 ± 28 MPa, respectively. The incorporation of 20 wt % ACC increased these values to 15.8 ± 0.93 GPa for the Young's modulus and 268 ± 20 MPa for the tensile strength. In these composites, $CaCO_3$, particularly Ca^{2+} ions serve as a cross-linking agent because of the ionic interactions with the carboxylate groups in CMC, CNFs, and PAA. The effects of these ionic interactions based on Ca^{2+} molecular interactions enhance the mechanical properties of the CMC/CNF/ACC composite films. In contrast, incorporation of 30 wt % ACC increased the Young's modulus to 18.0 ± 1.7 GPa and decreased the mechanical strength to 133 ± 2.4 MPa. This deterioration in the mechanical strength is presumably caused by the segregation of CMC/CNF and ACC domains in the CMC/CNF/ACC composite films. This observation suggests that a redundant amount of ACC results in mechanically weak materials because of the nature of ACC. These results show that ACC addition is an efficient tool for increasing the Young's modulus, although an excess of ACC leads to the formation of fragile composites.

The effects of ACC incorporation on the mechanical performance were studied by nanoindentation hardness testing

DOI: 10.1021/acsomega.8b02014
ACS Omega 2018, 3, 12722−12729

Table 2. Mechanical Properties of CMC/CNF and CMC Composite Materials with Various ACC Contents

	CMC/CNF/ACC (wt %)							
	50/50/0	45/45/10	40/40/20	35/35/30	100/0/0	87/0/13	80/0/20	71/0/29
Young's modulus (GPa)	10.7 ± 1.2	13.1 ± 2.3	15.8 ± 0.93	18.0 ± 1.7	3.0 ± 0.9	9.4 ± 0.9	11.6 ± 0.6	12.2 ± 1.4
tensile strength (MPa)	240 ± 28	260 ± 47	268 ± 20	133 ± 2.4	126 ± 39	250 ± 12	200 ± 14	97 ± 14

Table 3. Nanoindentation Hardness Testing Results for CMC/CNF with Various ACC Contents

	CMC/CNF/ACC (wt %)				
	100/0/0	50/50/0	45/45/10	40/40/20	35/35/30
indentation modulus (GPa)	6.6 ± 0.93	7.9 ± 2.2	8.9 ± 1.6	10.4 ± 2.2	16.7 ± 2.2
indentation hardness (GPa)	0.36 ± 0.02	0.39 ± 0.06	0.54 ± 0.17	0.74 ± 0.1	1.1 ± 0.15

(Table 3 and Figure S2). An increase in the amount of ACC in the CMC/CNF/ACC composites up to 30 wt % of ACC enhanced the modulus and hardness of the composite films. These results suggest that an appropriate amount of ACC interacting with the polymer fulfills the space between the organic matrices.

Mechanically tough transparent materials were achieved for the CMC/CNF/ACC composites. CMC plays key roles in the formation of homogeneous mixtures of CNFs and ACC in the solution mixing method. This method for synthesizing four-component composite films is an energy-efficient procedure for producing transparent composite films with sufficient tensile strength and indentation hardness. ACC has a key effect on the optical properties such as high transparency with tensile strength and hardness.

Comparison of Composites in the Presence and Absence of CNF. Transparent composite thin films composed of CMC and ACC, without CNFs, were prepared with ACC amounts, that is, 13, 20, and 29 wt %, similar to those in the CMC/CNF/ACC composites. FT-IR spectroscopy and XRD (Figures S3 and S4) confirmed that mixing of ACC/PAA and CMC solutions provided transparent amorphous CMC/ACC composite films. CMC and ACC/PAA colloids were homogeneously mixed by the solution mixing method, which was confirmed with the EDX analysis (Figure S5). The prepared CMC/ACC composite films showed high transparency in the wavelength region 300−800 nm (Figure S6). In contrast, UV−vis spectra of the CMC/CNF/ACC composites showed the light scattering at a wavelength of around 300 nm (Figure 4). This is caused by submicrometer-sized CNFs in the composite films. The transparencies in the visible-light region for the CNF-containing composites were comparable to those of composite films without CNF incorporation.

Mechanical tests were performed on CMC/ACC, and the mechanical properties were compared with those of the CMC/CNF/ACC composites. The dashed lines in Figure 6 show the results of tensile tests on the composite thin films containing 13, 20, and 29 wt % ACC in the CMC matrix, without CNFs. A summary of the mechanical properties of the composite films is given in Table 2. The effects of ACC incorporation on the mechanical properties of the CMC/ACC composites were similar to those in the case of CMC/CNF/ACC composites (Table 2). With respect to the effects of CNFs on the mechanical properties, it is clear that replacement of half of the CMC component in the CNF, that is, from 100/0/0 (CMC/CNF/ACC) to 50/50/0 (CMC/CNF/ACC), increased the Young's modulus three-fold and doubled the tensile strength (Table 2). For the composite films containing ACC, CNF replacement of half of the CMC component enhanced the mechanical strength. The incorporation of CNFs increased the Young's modulus and tensile strength values. Even in the presence of 30 wt % ACC, the replacement of CMC by CNFs, that is, from 71/0/29 (CMC/CNF/ACC) to 35/35/30 (CMC/CNF/ACC), increased both the Young's modulus and tensile strength ca. 1.5 times (Table 2). Although tensile strengths of the composite films without CNF incorporation were lower than those of the CMC/CNF/ACC composites, the elongation properties of CMC/ACC were higher than those of the CNF-containing composites. These results indicate that CNF introduction reduces elasticity and increases resistance to stretching.

The effects of CNFs on the mechanical properties were also examined by performing nanoindentation tests (Figure 7). A

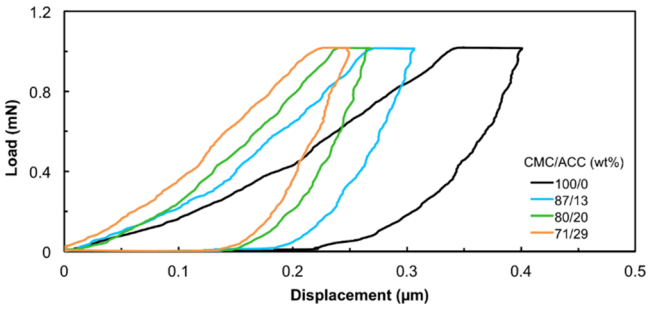

Figure 7. Indentation tests on the CMC material containing various weight percentages of ACC.

comparison of the indentation moduli and hardness values of 80/0/20 (CMC/CNF/ACC) and 40/40/20 (CMC/CNF/ACC) shows that CNF replacement of half of the CMC enhances the stiffness of the composite films (Tables 3 and 4). The incorporation of CNFs into CMC/ACC as a reinforcing material component showed significant effects on the mechanical strength of the composite.

It is demonstrated that the solution mixing method used in this study enables easy tuning of CMC/CNF/ACC content ratios, and these determine the mechanical properties of the composite films. The brief preparation process is advantageous for the development of environmentally friendly organic/inorganic composite materials with transparency and modulated mechanical performances. Zhu and his co-workers demonstrate that hot pressing of wood slices is a fast preparation method of cellulose-based films with high transparency of 90% and tensile strength of 150 MPa.[50] However, this useful method has not been used for the

DOI: 10.1021/acsomega.8b02014
ACS Omega 2018, 3, 12722−12729

Table 4. Nanoindentation Hardness Testing Results for CMC with Various ACC Contents

	CMC/ACC (wt %)			
	100/0	87/13	80/20	71/29
indentation modulus (GPa)	6.6 ± 0.93	8.3 ± 0.58	9.4 ± 0.32	15.4 ± 1.6
indentation hardness (GPa)	0.36 ± 0.02	0.59 ± 0.09	0.55 ± 0.14	1.0 ± 0.07

formation of composites with inorganic components, which can provide desired properties to cellulose-based films.

The results in the present study also suggest that the ACC incorporation into cellulose-based materials is an effective way to enhance the values of tensile strength and Young's modulus with maintaining high transparency and environmental friendliness. Although other inorganic components including clays have been utilized as additives to improve mechanical strength, the transparency at 600 nm is decreased to 40−80%.[51−56] The present CMC/CNF/ACC composite films exhibit around 90% of transparency at 600 nm, which is comparable to that of the state-of-the-art composite films based on CNFs with inorganic components.[57−59] In addition to the high transparency, 40/40/20 (CMC/CNF/ACC) showed 260 ± 20 MPa tensile strength and 15.8 ± 0.93 GPa Young's modulus, which are comparable to other tailor-made composite films based on CNFs.[51−53,58,59]

There are only a couple of reports on the development of CNF/ACC composite materials,[14,29] although ACC is a suitable component for the composite formation with CNFs because of the similar refractive index to cellulose materials. Gebauer et al. showed that the CNF/ACC coatings show high transparency.[29] The composite coatings show 0.27−0.41 GPa of indentation hardness, which is lower than the present CMC/CNF/ACC materials, and the formation of self-standing films has not been achieved.[29] To the best of our knowledge, only our previous report shows the formation of self-standing flexible CNF/ACC composite films.[14] In our previous report on transparent composites based on ACC and bacterial cellulose, an ACC colloidal suspension was percolated into the solid three-dimensional network of a cellulose hydrogel matrix. In the present report, we have shown advantages of using a water-dispersible polymeric crystalline cellulose derivative of CNFs as a matrix for mechanically tough composite films with high transparency and homogeneously dispersed ACC. For the materials obtained by the present method, molecular-scale interactions between cellulose derivatives and ACC through the intermolecular forces between carboxylate groups and Ca^{2+} ions enhance the stiffness of the flexible composite films. The Young's moduli of the CMC/CNF/ACC and CMC/ACC composite films are higher than those of composites based on the surface-carboxylated bacterial cellulose and ACC, 7.3 ± 0.5 GPa.[14] The tensile strengths of the composites in the present study are comparable to those of the composites in our previous study.[14]

The mechanical properties of the materials prepared in the present study are comparable to those of transparent composite films based on cellulose microfibrils and a clay mineral.[51−53,59] Structural control of the composite film is an effective approach to enhancement of mechanical properties. Alignment of CNFs is an efficient technique for enhancing the mechanical properties.[43,60] Furthermore, the chiral structures in the hard tissues of living organisms provide excellent mechanical toughness.[5,61] Further improvements in processing could lead to the development of transparent composite films, with enhanced mechanical properties, based on abundant natural resources.

CONCLUSIONS

We have developed transparent composite films composed of the cellulose derivatives, CMC and CNFs, and ACC, inspired by the composite structures in biominerals. Preparation of composite materials consisting of environmentally abundant materials and eco-friendly minerals was achieved with an energy-efficient procedure. The molecular-scale interactions between CMC and ACC endow the composite films with stiffness and hardness. The carboxylate groups of CMC, CNFs, and ACC generate electrostatic repulsion forces, which inhibit aggregation of two components. The four components form homogeneously dispersed structures in the composite film, leading to high mechanical strength and high transparency. Our biomineralization-inspired approaches can be applied for the formation of various organic/inorganic composite materials.[12,62,63] For example, calcium phosphate-based composite materials that have a potential for applications in a wide range of fields such as biomedical may be developed.[12,24,64] The present study promises that mimicking biomimetic structures could lead to the development of hard, strong, and transparent materials from abundant natural resources.

EXPERIMENTAL SECTION

Preparation of the CMC Solution. Dried sodium CMC powder (M_w = 100 000; etherification degree = 4 mmol g^{-1}; Nippon Paper Industries Co., Ltd., Tokyo, Japan) was stirred in water for 1 day at room temperature for the preparation of 5 wt % aqueous solution. The solution containing partially dissolved CMC was filtered to remove aggregated CMC chunks. The resultant CMC solution was dialyzed against distilled water to remove residual salts. The weight percentage of CMC in the solution was determined by gravimetric analysis.

Preparation of the ACC/PAA Precursor Solution. A colloidal suspension of the ACC/PAA precursor was prepared according to our previously reported method.[41] Anhydrous calcium chloride ($CaCl_2$) (Wako Pure Chemicals, Osaka, Japan) was added to an aqueous solution of PAA (M_w = 1.8 × 10^3; Aldrich, St Louis, MO, USA) to prepare a 0.1 M $CaCl_2$ solution containing 7.2 × 10^{-1} wt % PAA. An equal volume of a 0.1 M sodium carbonate (Na_2CO_3) (Kanto Chemical, Tokyo, Japan) solution was added to the $CaCl_2$/PAA solution. After reaction for 1 h, the ACC colloid was collected and washed by centrifugation. All chemical reagents were used without further purification.

Preparation of the CMC/CNF/ACC Composite Material. TEMPO-mediated oxidized CNFs (oxidization degree = 0.3 mmol g^{-1}; Nippon Paper Industries Co., Ltd., Tokyo, Japan) were homogeneously dispersed in deionized water at 0.5 wt %. The requisite ratios and amounts of CNFs and purified CMC were mixed with the purified ACC colloidal solution. After the four components were evenly dispersed and mixed, the solution was poured into a 3 cm × 6 cm ABS case and dried in an oven at 25 °C to obtain a freestanding film with the thickness of ca. 50 μm.

DOI: 10.1021/acsomega.8b02014
ACS Omega 2018, 3, 12722−12729

Preparation of the CMC/ACC Composite Material. The requisite amount of the purified CMC solution was homogeneously mixed with the ACC colloidal suspension. The prepared homogeneous dispersion was dried in an oven at 25 °C to form a transparent thin composite film.

Characterization. FT-IR spectroscopy was performed with a JASCO FT/IR-6100 spectrometer by the KBr method. The XRD patterns of the samples were recorded with Rigaku Smartlab (Rigaku, Tokyo, Japan) equipped with a monochromator-filtered Cu Kα radiation (λ = 0.154 nm) source at 40 kV and 40 mA. The UV−vis transmittance spectra were recorded with a JASCO V-670 (JASCO, Tokyo, Japan) spectrometer equipped with an integrating sphere unit (ISN-800T). The film and fracture surfaces were observed by SEM (Hitachi S-4700 scanning electron microscope, Hitachi High-Technologies, Tokyo, Japan). The SEM samples were coated with platinum, using a Hitachi E-1030 ion sputterer, before the SEM observations. EDX was performed at 10 kV with the Hitachi S-4700 SEM and a Horiba EMAX-7000 (Horiba, Kyoto, Japan) instrument. TEM was conducted with JEM-2010HC (JEOL Ltd., Tokyo, Japan) operated at 200 kV. The tensile strength tests were performed with a Shimadzu EZ-TEST instrument (Shimadzu, Kyoto, Japan) with a 500 N load cell. Rectangular specimens of width 5 mm and length 30 mm were prepared from the samples, and the tensile tests were conducted at a rate of 0.5 mm/min and a span length of 10 mm. The slope of the linear region of the stress−strain curve was used to determine the Young's modulus (E). To avoid the effects of moisture on the mechanical properties, the composite films were dried at 60 °C for 2 h before the tensile tests. The nanoindentation hardness was determined with a Shimadzu DUH-211SR (Shimadzu, Kyoto, Japan) instrument equipped with a Berkovich-shaped diamond tip. The force applied to the samples was 1 mN.

■ ASSOCIATED CONTENT

Supporting Information

The Supporting Information is available free of charge on the ACS Publications website at DOI: 10.1021/acsomega.8b02014.

TEM image of the CNF network; nanoindentation curves for the CMC/CNF/ACC composite materials at various ACC contents; XRD patterns and the FT-IR spectra of the CMC/ACC composite materials; EDX results of the CMC/ACC composite; and UV−vis spectra of the CMC/ACC composites (PDF)

■ AUTHOR INFORMATION

Corresponding Author

*E-mail: kato@chiral.t.u-tokyo.ac.jp (T.K.).

ORCID

David Kuo: 0000-0002-5603-4379
Tatsuya Nishimura: 0000-0002-8416-4007
Satoshi Kajiyama: 0000-0002-2200-7524
Takashi Kato: 0000-0002-0571-0883

Present Address

†Division of Material Sciences, Kanazawa University, Kakuma-machi, Kanazawa, Ishikawa, 920-1192 Japan.

Notes

The authors declare no competing financial interest.

■ ACKNOWLEDGMENTS

We are grateful for the experimental support from Kotaro Ito and Dai Nagahara of the Nippon Paper Industries Co., Ltd. This study was partly financially supported by KAKENHI 15H02179. TEM observation of samples was conducted at Advanced Characterization Nanotechnology Platform of the University of Tokyo, supported by "Nanotechnology Platform" of the MEXT, Japan. We thank Helen McPherson, PhD, from Edanz Group (www.edanzediting.com/ac) for editing a draft of this manuscript.

■ REFERENCES

(1) *Handbook of Biomineralization*; Bauerlein, E., Ed.; Wiley-VCH: Weinheim, 2007.

(2) Mann, S. *Biomineralization Principles and Concepts in Bioinorganic Materials Chemistry*; Oxford University Press: Oxford, 2001.

(3) Sanderson, K. Structure: Artificial Armour. *Nature* **2015**, *519*, S14−S15.

(4) Kato, T.; Sakamoto, T.; Nishimura, T. Macromolecular Templating for the Formation of Inorganic-Organic Hybrid Structures. *MRS Bull.* **2010**, *35*, 127−132.

(5) Grunenfelder, L. K.; Herrera, S.; Kisailus, D. Crustacean-Derived Biomimetic Components and Nanostructured Composites. *Small* **2014**, *10*, 3207−3232.

(6) Nudelman, F.; Sommerdijk, N. A. J. M. Biomineralization as an Inspiration for Materials Chemistry. *Angew. Chem., Int. Ed.* **2012**, *51*, 6582−6596.

(7) Meldrum, F. C.; Cölfen, H. Controlling Mineral Morphologies and Structures in Biological and Synthetic Systems. *Chem. Rev.* **2008**, *108*, 4332−4432.

(8) Arakaki, A.; Shimizu, K.; Oda, M.; Sakamoto, T.; Nishimura, T.; Kato, T. Biomineralization-Inspired Synthesis of Functional Organic/Inorganic Hybrid Materials: Organic Molecular Control of Self-Organization of Hybrids. *Org. Biomol. Chem.* **2015**, *13*, 974−989.

(9) Kato, T.; Sugawara, A.; Hosoda, N. Calcium Carbonate-Organic Hybrid Materials. *Adv. Mater.* **2002**, *14*, 869−877.

(10) Cantaert, B.; Kuo, D.; Matsumura, S.; Nishimura, T.; Sakamoto, T.; Kato, T. Use of Amorphous Calcium Carbonate for the Design of New Materials. *ChemPlusChem* **2017**, *82*, 107−120.

(11) Matsumura, S.; Kajiyama, S.; Nishimura, T.; Kato, T. Formation of Helically Structured Chitin/$CaCO_3$ Hybrids through an Approach Inspired by the Biomineralization Processes of Crustacean Cuticles. *Small* **2015**, *11*, 5127−5133.

(12) Nakayama, M.; Kajiyama, S.; Kumamoto, A.; Nishimura, T.; Ikuhara, Y.; Yamato, M.; Kato, T. Stimuli-Responsive Hydroxyapatite Liquid Crystal with Macroscopically Controllable Ordering and Magneto-Optical Functions. *Nat. Commun.* **2018**, *9*, 568.

(13) Mao, L.-B.; Gao, H.-L.; Yao, H.-B.; Liu, L.; Colfen, H.; Liu, G.; Chen, S.-M.; Li, S.-K.; Yan, Y.-X.; Liu, Y.-Y.; Yu, S.-H. Synthetic Nacre by Predesigned Matrix-Directed Mineralization. *Science* **2016**, *354*, 107−110.

(14) Saito, T.; Oaki, Y.; Nishimura, T.; Isogai, A.; Kato, T. Bioinspired Stiff and Flexible Composites of Nanocellulose-Reinforced Amorphous $CaCO_3$. *Mater. Horiz.* **2014**, *1*, 321−325.

(15) Okumura, K. Strength and Toughness of Biocomposites Consisting of Soft and Hard Elements: A Few Fundamental Models. *MRS Bull.* **2015**, *40*, 333−339.

(16) Zhao, Y.; Luo, Z.; Li, M.; Qu, Q.; Ma, X.; Yu, S.-H.; Zhao, Y. A Preloaded Amorphous Calcium Carbonate/Doxorubicin@Silica Nanoreactor for pH-Responsive Delivery of an Anticancer Drug. *Angew. Chem., Int. Ed.* **2015**, *54*, 919−922.

(17) Mayer, G. Rigid Biological Systems as Models for Synthetic Composites. *Science* **2005**, *310*, 1144−1147.

(18) Munch, E.; Launey, M. E.; Alsem, D. H.; Saiz, E.; Tomsia, A. P.; Ritchie, R. O. Tough, Bio-Inspired Hybrid Materials. *Science* **2008**, *322*, 1516−1520.

DOI: 10.1021/acsomega.8b02014
ACS Omega 2018, 3, 12722−12729

(19) Lei, Z.; Wang, Q.; Sun, S.; Zhu, W.; Wu, P. A Bioinspired Mineral Hydrogel as a Self-Healable, Mechanically Adaptable Ionic Skin for Highly Sensitive Pressure Sensing. *Adv. Mater.* **2017**, *29*, 1700321.
(20) Kuwabara, K.; Oaki, Y.; Muramatsu, R.; Imai, H. Crystal-Surface-Induced Simultaneous Synthesis and Hierarchical Morphogenesis of Conductive Polymers. *Chem. Commun.* **2015**, *51*, 9698−9701.
(21) Oaki, Y. Morphology Design of Crystalline and Polymer Materials from Nanoscopic to Macroscopic Scales. *Bull. Chem. Soc. Jpn.* **2017**, *90*, 776−788.
(22) He, M.; Wang, X.; Wang, Z.; Chen, L.; Lu, Y.; Zhang, X.; Li, M.; Liu, Z.; Zhang, Y.; Xia, H.; Zhang, L. Biocompatible and Biodegradable Bioplastics Constructed from Chitin via a "Green" Pathway for Bone Repair. *ACS Sustainable Chem. Eng.* **2017**, *5*, 9126−9135.
(23) Kawata, M.; Azuma, K.; Izawa, H.; Morimoto, M.; Saimoto, H.; Ifuku, S. Biomineralization of Calcium Phosphate Crystals on Chitin Nanofiber Hydrogel for Bone Regeneration Material. *Carbohydr. Polym.* **2016**, *136*, 964−969.
(24) Pangon, A.; Saesoo, S.; Saengkrit, N.; Ruktanonchai, U.; Intasanta, V. Hydroxyapatite-Hybridized Chitosan/Chitin Whisker Bionanocomposite Fibers for Bone Tissue Engineering Applications. *Carbohydr. Polym.* **2016**, *144*, 419−427.
(25) Xiao, C.; Li, M.; Wang, B.; Liu, M.-F.; Shao, C.; Pan, H.; Lu, Y.; Xu, B.-B.; Li, S.; Zhan, D. Total Morphosynthesis of Biomimetic Prismatic-Type $CaCO_3$ Thin Films. *Nat. Commun.* **2017**, *8*, 1398.
(26) Nagai, Y.; Oaki, Y.; Imai, H. Artificial Mineral Films Similar to Biogenic Calcareous Shells: Oriented Calcite Nanorods on a Self-Standing Polymer Sheet. *CrystEngComm* **2018**, *20*, 1656−1661.
(27) Li, M.; Chen, Y.; Mao, L.-B.; Jiang, Y.; Liu, M.-F.; Huang, Q.; Yu, Z.; Wang, S.; Yu, S.-H.; Lin, C.; Liu, X. Y.; Cölfen, H. Seeded Mineralization Leads to Hierarchical $CaCO_3$ Thin Coatings on Fibers for Oil/Water Separation Applications. *Langmuir* **2018**, *34*, 2942−2951.
(28) Matsumura, S.; Horiguchi, Y.; Nishimura, T.; Sakai, H.; Kato, T. Biomineralization-Inspired Preparation of Zinc Hydroxide Carbonate/Polymer Hybrids and Their Conversion into Zinc Oxide Thin-Film Photocatalysts. *Chem.—Eur. J.* **2016**, *22*, 7094−7101.
(29) Gebauer, D.; Oliynyk, V.; Salajkova, M.; Sort, J.; Zhou, Q.; Bergström, L.; Salazar-Alvarez, G. A Transparent Hybrid of Nanocrystalline Cellulose and Amorphous Calcium Carbonate Nanoparticles. *Nanoscale* **2011**, *3*, 3563−3566.
(30) Walther, A.; Bjurhager, I.; Malho, J.-M.; Pere, J.; Ruokolainen, J.; Berglund, L. A.; Ikkala, O. Large-Area, Lightweight and Thick Biomimetic Composites with Superior Material Properties Via Fast, Economic, and Green Pathways. *Nano Lett.* **2010**, *10*, 2742−2748.
(31) Yao, H.-B.; Fang, H.-Y.; Wang, X.-H.; Yu, S.-H. Hierarchical Assembly of Micro-/Nano-Building Blocks: Bio-Inspired Rigid Structural Functional Materials. *Chem. Soc. Rev.* **2011**, *40*, 3764−3785.
(32) Sung, K.; Nakagawa, S.; Yoshie, N. Fabrication of Water-Resistant Nacre-Like Polymer/Clay Nanocomposites via in Situ Polymerization. *ACS Omega* **2017**, *2*, 8475−8482.
(33) Addadi, L.; Raz, S.; Weiner, S. Taking Advantage of Disorder: Amorphous Calcium Carbonate and Its Roles in Biomineralization. *Adv. Mater.* **2003**, *15*, 959−970.
(34) Meldrum, F. C. Calcium Carbonate in Biomineralisation and Biomimetic Chemistry. *Int. Mater. Rev.* **2003**, *48*, 187−224.
(35) Aizenberg, J.; Tkachenko, A.; Weiner, S.; Addadi, L.; Hendler, G. Calcitic Microlenses as Part of the Photoreceptor System in Brittlestars. *Nature* **2001**, *412*, 819−822.
(36) Beniash, E.; Aizenberg, J.; Addadi, L.; Weiner, S. Amorphous Calcium Carbonate Transforms into Calcite During Sea Urchin Larval Spicule Growth. *Proc. R. Soc. B* **1997**, *264*, 461−465.
(37) Aizenberg, J.; Addadi, L.; Weiner, S.; Lambert, G. Stabilization of Amorphous Calcium Carbonate by Specialized Macromolecules in Biological and Synthetic Precipitates. *Adv. Mater.* **1996**, *8*, 222−226.
(38) Aizenberg, J.; Muller, D. A.; Grazul, J. L.; Hamann, D. R. Direct Fabrication of Large Micropatterned Single Crystals. *Science* **2003**, *299*, 1205−1208.
(39) Raz, S.; Hamilton, P. C.; Wilt, F. H.; Weiner, S.; Addadi, L. The Transient Phase of Amorphous Calcium Carbonate in Sea Urchin Larval Spicules: The Involvement of Proteins and Magnesium Ions in Its Formation and Stabilization. *Adv. Funct. Mater.* **2003**, *13*, 480−486.
(40) Nakayama, M.; Kajiyama, S.; Nishimura, T.; Kato, T. Liquid-Crystalline Calcium Carbonate: Biomimetic Synthesis and Alignment of Nanorod Calcite. *Chem. Sci.* **2015**, *6*, 6230−6234.
(41) Oaki, Y.; Kajiyama, S.; Nishimura, T.; Imai, H.; Kato, T. Nanosegregated Amorphous Composites of Calcium Carbonate and an Organic Polymer. *Adv. Mater.* **2008**, *20*, 3633−3637.
(42) Zhang, J.; Luo, N.; Wan, J.; Xia, G.; Yu, J.; He, J.; Zhang, J. Directly Converting Agricultural Straw into All-Biomass Nanocomposite Films Reinforced with Additional in Situ-Retained Cellulose Nanocrystals. *ACS Sustainable Chem. Eng.* **2017**, *5*, 5127−5133.
(43) Zhu, M.; Wang, Y.; Zhu, S.; Xu, L.; Jia, C.; Dai, J.; Song, J.; Yao, Y.; Wang, Y.; Li, Y.; Henderson, D.; Luo, W.; Li, H.; Minus, M. L.; Li, T.; Hu, L. Anisotropic, Transparent Films with Aligned Cellulose Nanofibers. *Adv. Mater.* **2017**, *29*, 1606284.
(44) Henriksson, M.; Berglund, L. A.; Isaksson, P.; Lindström, T.; Nishino, T. Cellulose Nanopaper Structures of High Toughness. *Biomacromolecules* **2008**, *9*, 1579−1585.
(45) Kang, X.; Sun, P.; Kuga, S.; Wang, C.; Zhao, Y.; Wu, M.; Huang, Y. Thin Cellulose Nanofiber from Corncob Cellulose and Its Performance in Transparent Nanopaper. *ACS Sustainable Chem. Eng.* **2017**, *5*, 2529−2534.
(46) Zhu, H.; Fang, Z.; Preston, C.; Li, Y.; Hu, L. Transparent Paper: Fabrications, Properties, and Device Applications. *Energy Environ. Sci.* **2014**, *7*, 269−287.
(47) Borodin, V. L.; Nefedova, I. V. Growth and Characteristics of Calcite Single Crystals. *J. Cryst. Growth* **2005**, *275*, e633−e636.
(48) Okumura, T.; Ishikawa, T.; Koike, Y.; Tagaya, A. Scattering Polarizer with Anisotropic Crystals in a Polyolefin Polymer. *Appl. Phys. Lett.* **2003**, *82*, 496−498.
(49) Yano, H.; Sugiyama, J.; Nakagaito, A. N.; Nogi, M.; Matsuura, T.; Hikita, M.; Handa, K. Optically Transparent Composites Reinforced with Networks of Bacterial Nanofibers. *Adv. Mater.* **2005**, *17*, 153−155.
(50) Zhu, M.; Jia, C.; Wang, Y.; Fang, Z.; Dai, J.; Xu, L.; Huang, D.; Wu, J.; Li, Y.; Song, J.; Yao, Y.; Hitz, E.; Wang, Y.; Hu, L. Istropic Paper Directly from Anistropic Wood: Top-down Green Transparent Substrate Toward Biodegradable Electronics. *ACS Appl. Mater. Interfaces* **2018**, *10*, 28566.
(51) Sehaqui, H.; Liu, A.; Zhou, Q.; Berglund, L. A. Fast Preparation Procedure for Large, Flat Cellulose and Cellulose/Inorganic Nanopaper Structures. *Biomacromolecules* **2010**, *11*, 2195−2198.
(52) Aulin, C.; Salazar-Alvarez, G.; Lindström, T. High Strength, Flexible and Transparent Nanofibrillated Cellulose-Nanoclay Biohybrid Films with Tunable Oxygen and Water Vapor Permeability. *Nanoscale* **2012**, *4*, 6622−6628.
(53) Das, P.; Schipmann, S.; Malho, J.-M.; Zhu, B.; Klemradt, U.; Walther, A. Facile Access to Large-Scale, Self-Assembled, Nacre-Inspired, High-Performance Materials with Tunable Nanoscale Periodicities. *ACS Appl. Mater. Interfaces* **2013**, *5*, 3738−3747.
(54) Wu, C.-N.; Saito, T.; Fujisawa, S.; Fukuzumi, H.; Isogai, A. Ultrastrong and High Gas-Barrier Nanocellulose/Clay-Layered Composites. *Biomacromolecules* **2012**, *13*, 1927−1932.
(55) Nissinen, T.; Li, M.; Davis, S. A.; Mann, S. In Situ Precipitation of Amorphous and Crystalline Calcium Sulphates in Cellulose Thin Films. *CrystEngComm* **2014**, *16*, 3843−3847.
(56) Cui, P.; Parida, K.; Lin, M.-F.; Xiong, J.; Cai, G.; Lee, P. S. Transparent, Flexible Cellulose Nanofibril-Phosphorene Hybrid Paper as Triboelectric Nanogenerator. *Adv. Mater. Interfaces* **2017**, *4*, 1700651.

DOI: 10.1021/acsomega.8b02014
ACS Omega 2018, 3, 12722−12729

(57) Ming, S.; Chen, G.; He, J.; Kuang, Y.; Liu, Y.; Tao, R.; Ning, H.; Zhu, P.; Liu, Y.; Fang, Z. Highly Transparent and Self-Extinguishing Nanofibrillated Cellulose-Monolayer Clay Nanoplatelet Hybrid Films. *Langmuir* **2017**, *33*, 8455−8462.
(58) Ji, S.; Jang, J.; Cho, E.; Kim, S.-H.; Kang, E.-S.; Kim, J.; Kim, H.-K.; Kong, H.; Kim, S.-K.; Kim, J.-Y.; Park, J.-U. High Dielectric Performances of Flexible and Transparent Cellulose Hybrid Films Controlled by Multidimensional Metal Nanostructures. *Adv. Mater.* **2017**, *29*, 1700538.
(59) Liu, Y.; Yu, S.-H.; Bergström, L. Transparent and Flexible Nacre-Like Hybrid Films of Aminoclays and Carboxylated Cellulose Nanofibrils. *Adv. Funct. Mater.* **2018**, *28*, 1703277.
(60) Cai, J.; Chen, J.; Zhang, Q.; Lei, M.; He, J.; Xiao, A.; Ma, C.; Li, S.; Xiong, H. Well-Aligned Cellulose Nanofiber-Reinforced Polyvinyl Alcohol Composite Film: Mechanical and Optical Properties. *Carbohydr. Polym.* **2016**, *140*, 238−245.
(61) Raabe, D.; Sachs, C.; Romano, P. The Crustacean Exoskeleton as an Example of a Structurally and Mechanically Graded Biological Nanocomposite Material. *Acta Mater.* **2005**, *53*, 4281−4292.
(62) Kajiyama, S.; Sakamoto, T.; Inoue, M.; Nishimura, T.; Yokoi, T.; Ohtsuki, C.; Kato, T. Rapid and Topotactic Transformation from Octacalcium Phosphate to Hydroxyapatite (HAP): A New Approach to Self-Organization of Free-Standing Thin-Film HAP-Based Nanohybrids. *CrystEngComm* **2016**, *18*, 8388−8395.
(63) Han, Y.; Nishimura, T.; Iimura, M.; Sakamoto, T.; Ohtsuki, C.; Kato, T. Periodic Surface-Ring Pattern Formation for Hydroxyapatite Thin Films Formed by Biomineralization-Inspired Processes. *Langmuir* **2017**, *33*, 10077−10083.
(64) Iijima, K.; Sakai, A.; Komori, A.; Sakamoto, Y.; Matsuno, H.; Serizawa, T.; Hashizume, M. Control of Biomimetic Hydroxyapatite Deposition on Polymer Substrates Using Different Protein Adsorption Abilities. *Colloids Surf., B* **2015**, *130*, 77−83.

DOI: 10.1021/acsomega.8b02014
ACS Omega 2018, 3, 12722−12729